

Maxillary-arch Shape Associated with the Position of the Greater Palatine Foramen

Margot de los Ríos Argumedo¹, Hanny Gonzales-Olaza², Dian Agustin Wahjuningrum^{3*}, Amanda⁴, Violeta Malpartida-Carrillo⁵, Maria Eugenia Guerrero⁶

1. Faculty of Dentistry, Universidad Nacional Federico Villareal, Lima, Perú.

2. Faculty of Health of Sciences, Postgraduate Department, Universidad Científica Del Sur, Lima, Perú .

3. Department of Conservative Dentistry, Faculty of Dental Medicine, Universitas Airlangga, Indonesia.

4. Resident of Conservative Dentistry Specialist, Faculty of Dental Medicine, Universitas Airlangga, Surabaya.

5. School of Stomatology, Universidad Privada San Juan Bautista, Lima, Perú.

6. Department of Medico Surgical Stomatology, Faculty of Dentistry, Universidad Nacional Mayor de San Marcos, Lima, Perú.

Abstract

An observational study was carried out on 103 CBCTs. The GPF position was assessed by drawing guidelines in the CBCT axial image located between the first, second and third molar and in the center of the second and third molar, performing five guidelines on each side. Also, the depths and widths of the dental arches were measured at the canine and second molar regions to determine maxillary arch shapes (ovoid, square and tapered) by calibrated interexaminers (Kappa index and Intraclass correlation coefficient). An association test was performed using the Chi-square Pearson test and the Fisher exact test ($P < 0.05$).

Objectives to determine the association of the maxillary arch shape with the greater palatine foramen (GPF) position using CBCT scans.

Position C (68.94%) was the most frequent position followed by position B (19.42%), position D (7.76%), and position E (3.88%). Hence, 76.70% of the GPFs were located in the opposite to the third molars position. The Fisher's exact test showed a significant association between position C and all age groups ($P < 0.001$). The ovoid maxillary arch was the most frequent in teeth of female patients (27.18%) followed by males (23.31%). Position C was mostly frequent in ovoid (33.98%), square (33.31%), and tapered (11.64%) arches. However, the Chi-square Pearson test did not show a significant association between these variables ($P = 0.332$).

The shape of the maxillary arch and the position of the GPF had no association.

Clinical article (J Int Dent Med Res 2022; 15(1): 165-171)

Keywords: Anatomy, Cone-beam computed tomography, dental arch, hard palate, patient satisfaction.

Received date: 15 January 2022

Accept date: 02 March 2022

Introduction

Smiles become not only the focal point of people's attention but also as a key feature of the overall aesthetic appearance. Free gingival graft and connective tissue graft harvesting from the palate has provided a reliable approach for increasing the keratinized tissue width around the teeth and implants, augmenting gingival thickness, and treating gingival recessions for improving the aesthetic.¹ Intraoperative and postoperative bleeding caused by injuries to the

palatal vessels is one of the most common complications in these procedures.² Hence, comprehensive knowledge of anatomy is necessary for reducing the risk of complications.

It has been reported that the anatomy of the palatal vault strongly influenced the risk of injury of the greater palatine artery (GPA).³ If a haemorrhage occurs in the GPA, it is more complicated to perform haemostasis or ligation of the vessel, leaving only the placement of bone wax making compression. Besides, the greater palatine nerve (GPN) emerges through the greater palatine foramen (GPF) allowing the maxillary nerve block anesthetic technique (on the entire hemi-maxilla, including teeth, palatal and gingival mucosa, the midface area, maxillary sinus, and nasal cavity).⁴ Therefore, the position of the GPF is important to avoid haemorrhagic risks and anesthetic failures.

*Corresponding author:

Dian Agustin Wahjuningrum
Faculty of Dental Medicine, Universitas Airlangga
St. Prof. Dr Moestopo 47, Surabaya- East Java. Indonesia.
E-mail: dian-agustin-w@fkg.unair.ac.id

The position of the GPF, the course of the GPA, the distance from the GPF to the anterior nasal spine, to the posterior border of the hard palate and to the mid palatine suture as well as to the cement enamel junction of the teeth have been assessed in several cadaveric studies.⁵⁻⁷ In African and Indian populations, the GPF was found at the third molars.^{8,9} The GPF was also located in the third molars of white^{3,10} and South American populations (Brazilian).^{11,12} However, studies from Asia have reported that the GPF was localized at the second molar¹³ or between the second and the third molars.¹⁴ Previous studies have also included variations in the geometry of the GPF likely due to the size of the maxillary arch and the craniofacial ethnic differences.^{15,16}

In 2001, Noroozi et al.¹⁷ proposed a mathematical model for the human dental arch and identified the square, ovoid, and tapered arches. Four years later, Kook et al.¹⁸ evaluated mandibular arches using dental models and indicated that the most prevalent arch forms in Korean and North American populations were the square and the tapered ones, respectively. Cone-beam computed tomography (CBCT) is used as a non-invasive technique to evaluate human

dental arch forms as tools for detailed and accurate bone assessments.¹⁹⁻²³ This may contribute to clinical decisions when clinicians plan gingival graft and connective tissue graft harvesting. The literature search failed to find any publications concerning maxillary arch forms and GPF. Hence, to address the lack of publications on these variables, this current study assessed the association between the maxillary arch forms and the position of GPF using CBCT scans.

Materials and methods

Research Samples

One hundred and three CBCT images from Peruvian adults aged 18 to 77 years (51 men and 52 women) were selected from the records of the Diagnostic Imaging Centre in 2018. All the patients were informed that the CBCT scans would be anonymously used for research purposes later and were requested to sign informed consent forms.

Research Methods

This study only included CBCT images from subjects with the presence of maxillary canines and fully erupted molars at least on one

side and the absence of any pathological condition or deformities of the jaws. Edentulous patients, who had undergone orthodontic corrections, and those with crowns or metallic structures that could generate artifacts near the anatomical structures, incomplete clinical records, and distorted images were excluded from the research samples.

All CBCTs were taken with the same equipment, Point 3D Combi 500S (PointNix, Hwaseong, Seoul, South Korea) set to 5 mA, 90 Kv, a voxel of 0.23 mm, and the field of view of 120 x 90 mm and 140 x 90 mm. The scanning took 19 seconds to complete. The images were always obtained from patients in a standing position with the head positioned straight by the device in which the mid-sagittal plane was perpendicular to the floor plane and parallel to the Camper's plane. The multi-planar reconstruction images were generated by the Real Scan software (PointNix, Hwaseong, Seoul, South Korea) and were analysed in a Samsung Intel Core i7-4770 workstation. Images were viewed in a dimly lit room on an 18-inch monitor (Toshiba monitor, Tokyo, Japan) set at a screen resolution of 1366 x 768 and 32-bit colour depth.

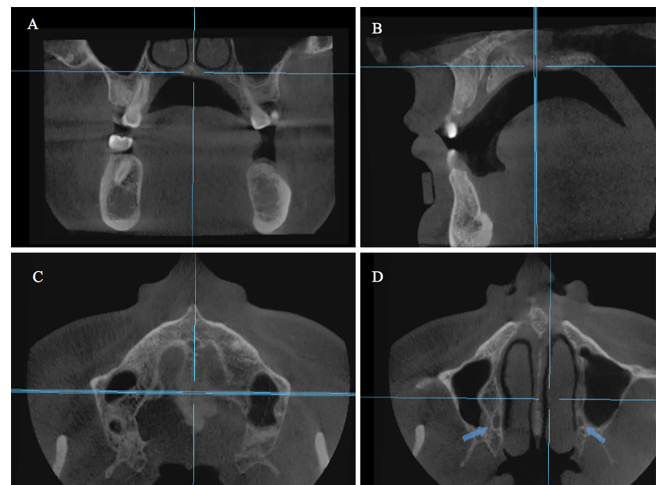


Figure 1. A. Coronal CBCT image shows the intersection of the midsagittal plane with the nasal cavity floor plane. B&C. Sagittal and axial CBCT image shows the midsagittal plane and the long axis of the nasal cavity floor plane selected to obtain a proper axial view of the anterior and posterior nasal spine. D. Axial CBCT image shows the right and left GPF.

The images were acquired at stages as follows. First, the midsagittal plane and the nasal cavity floor plane were selected on the coronal

view. Second, the midsagittal plane and the long axis of the palatal plane were selected on the sagittal view with both the anterior and posterior nasal spines in the same horizontal plane to obtain a proper axial view of the nasopalatine canal (Figure 1).

Greater palatine foramen position

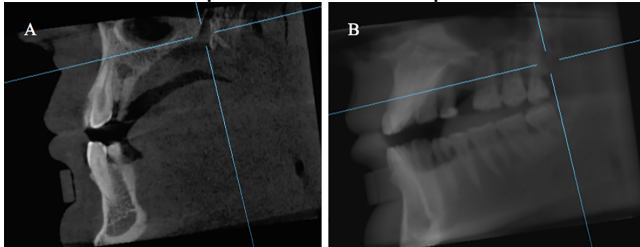


Figure 2. A. Sagittal CBCT shows the opening of GPF using a small thickness cut. B. Sagittal CBCT shows the GPF position distally to the third molar using a full thickness cut.

To assess the position of the GPF related to the upper molars, evaluation was conducted on each image in axial reconstruction considering the classification proposed by Ikuta et al.¹² Once the centre of the GPF was located, five tangents were drawn parallel to the middle of and interproximal to the face of the maxillary molars. The following classification was used to assess the positions: (A) from the medial surface of the second molar to its centre; (B) from the centre of the second molar up to its distal face; (C) from the medial surface of the third molar up to its centre; (D) from the centre of the third molar up to its distal face; and (E) distal from the third molar. A new depth of the axial reconstruction demonstrated an overlap between the previous tangents with the GPF, and thus it was possible to evaluate the relationship between upper molars and GPF. The exact position of the GPF showed an overlap with the tangents drawn, and this image of the position was recorded as JPEG (Figure 2).

Arch forms

To measure arch forms, an axial view considered the incisal edges, canines, and molar cusps. The depths and widths of the dental arches at the canines and second molar regions were measured using the formula initiated by Noroozi et al.¹⁷ The depths and widths were defined as follows: 1. Intersecond molar width (Wm): the distance between the distobuccal cusp tips of the second molars; 2. Intercanine width (Wc): the distance between the canine cusp tips; 3. Second molar depth (Dm): the distance

between the contact of the central incisors and a line that connects the distobuccal cusp tips of the second molars; 4. Canine depth (Dc): the distance between the contact of the central incisors and a line that connects the canine cusp tips.

The $(Wc/Wm) \times (Dc/Dm) - 1$ ratio could describe the arch forms. When this ratio of a dental arch was within the range of mean \pm 1 SD (standard deviation), the arch could be considered ovoid. However, when this ratio was more than mean + 1 SD, the arch form could be considered square. Finally, when this ratio was less than mean + 1 SD, an arch form could be tapered.

Reliability

All measurements and variable assessments were taken by two observers, one oral maxillofacial radiologist with more than 10year experience and one periodontist previously calibrated by the oral maxillofacial radiologist. Intra- and inter-examiner reliability was evaluated with the Kappa index, obtaining values greater than 0.8 for all qualitative parameters (95% confidence interval: 0.80-1.00). Quantitative measurements were evaluated using the intraclass correlation coefficient, obtaining values greater than 0.90 for all measurements (95% confidence interval: 0.90-0.99). Additionally, Dahlberg's errors were smaller than 0.8 mm (from 0.5 to 0.8) for these measurements. All variables were re-measured after a 30-day interval.

Statistical methods

Statistical analyses were performed using the Stata 14.0 (StataCorp LP, College Station, TX, USA). Normal distribution was confirmed using the Shapiro-Wilk test. Associations between qualitative variables were evaluated using the Chi-square Pearson's test or Fisher's exact test. The significance level was set at $P < 0.05$.

Results

A total of 103 (100%) CBCTs distributed into three age groups: (1) from 18 to 40 years (43.69%), (2) from 41 to 60 years of age (41.5%), (3) from 61 to 77 years (14.56%), were included for analysis. Viewed from gender, the position C of GPF (68.94%) was more frequently found in males (35.92%) than females (33.02%), followed by position B (19.42%), position D (7.76%),

position E (3.88%) and position A (0%).

Gender	A n (%)	B n (%)	C n (%)	D n (%)	E n (%)	Total n (%)	P Value
Male	0	10 (9.71)	37 (35.92)	3 (2.91)	1 (0.97)	51 (49.51%)	0.696
Female	0	10 (9.71)	34 (33.02)	5 (4.85)	3 (2.91)	52 (50.49%)	
Total	0	20 (19.42)	71 (68.94)	8 (7.76)	4 (3.88)	n=103	

Table 1. Position of GPF in relation to maxillary molar teeth considering gender.

The Fisher's exact test did not show a significant association between the position of GPF (Greater palatine foramen) and gender (P=0.696) (Table 1). According to age, position C was mostly seen in the age group of 41-60 years (36.90%), followed by the age groups of 18-40 years (21.36%) and 61-77 years (10.68%).

Age stages	A n (%)	B n (%)	C n (%)	D n (%)	E n (%)	Total n (%)	P Value
18 - 40 years	0	17 (16.51)	22 (21.36)	4 (3.88)	2 (1.94)	45 (43.69%)	<0.001
41 - 60 years	0	1 (0.97)	38 (36.90)	2 (1.94)	2 (1.94)	43 (41.75%)	
61 - 77 years	0	2 (1.94)	11 (10.68)	2 (1.94)	0	15 (14.56%)	
Total	0	20 (19.42)	71 (68.94)	8 (7.76)	4 (3.88)	n=103	

Table 2. Position of GPF in relation to maxillary molar teeth considering age stages.

The Fisher's exact test showed a significant association between position C and all age groups (P<0.001) (Table 2). In relation to dental arch forms by gender, ovoid dental arches were more dominantly found in females (27.18%) than males (23.31%).

Gender	Ovoid	Square	Tapered	Total	P Value
Male	24 (23.31)	21 (20.38)	06 (5.82)	51 (49.51%)	0.672
Female	28 (27.18)	17 (16.51)	07 (6.80)	52 (50.49%)	
Total	52 (50.49)	38 (36.89)	13 (12.62)	n= 103	

Table 3. Dental arch shape in relation to maxillary molar teeth considering gender.

The Chi-square Pearson's test did not show a significant association between the dental arch forms and gender (P=0.672) (Table 3). While, regarding age, ovoid arches were more frequently captured in the age group of 18-40 years (23.31%) compared to the age group of 41-60 years (21.36%). Lastly, tapered arches were the least frequently found in patients aged 61-77 years (0.98%).

Age stages	Ovoid	Square	Tapered	Total	P Value
18 - 40 years	24 (23.31)	15 (14.56)	6 (5.82)	45 (43.69%)	0.698
41 - 60 years	22 (21.36)	15 (14.56)	6 (5.82)	43 (41.74%)	
61 - 77 years	06 (5.82)	08 (7.77)	1 (0.98)	15 (14.57%)	
Total	52 (50.49)	38 (36.89)	13 (12.62%)	n=103	

Table 4. Dental arch shape in relation to maxillary molar teeth considering ages stages.

The Chi-square Pearson's test did not show a significant association between dental arch forms and age groups (P=0.698) (Table 4). Considering the position of the GPF related to the maxillary arch forms, position C was most frequently observed in ovoid (33.98%), square (33.31%), and tapered (11.64%) arches.

Arch form	A n (%)	B n (%)	C n (%)	D n (%)	E n (%)	Total	P value
Ovoid	0	12 (11.65)	35 (33.98)	4 (3.88)	1 (0.98)	52 (50.49%)	0.332
Square	0	8 (7.77)	24 (23.31)	3 (2.91)	3 (2.91)	38 (36.89%)	
Tapered	0	0	12 (11.64)	1 (0.98)	0	13 (12.62%)	
Total	0	20 (19.42)	71 (68.93)	8 (7.77)	4 (3.89)	103	

Table 5. Association between the position of the GPF with the maxillary arch shape.

However, the Chi-square Pearson's test did not show a significant association between these variables (P=0.332) (Table 5).

Discussion

An accurate assessment of anatomical structures positions such as the GPF has substantial clinical relevance in periodontal plastic surgery, maxillofacial surgery, and general dentistry. There is much information about the position of the GPF on dry skulls, and certain variations in different populations are documented. However, one of the major limitations of investigations on dry skulls is that those studies did not take gender and age into account while and these are important variables due to the sexual dimorphism.³ To add new insights against these limitations, technological advances of imaging techniques such as the computed tomography (CT),^{3,24} CBCT,^{12,16,25,27} and micro-CT,⁷ have been proposed for more detailed and accurate assessments of GPF and adjacent structures.

Several studies used dry skulls for identifying the positions of the GPF. In Nigerian populations, the GPF was between the mesial surface and the centre in 40% of the cases and opposite to the third molars in 8.46% of the cases⁸ Besides, other studies have stated that the GPF was located at the third molars in 76%

of the cases,²⁷ and distal to the midpalate region of the third molars in 96% of African cases.²⁸ The pooled prevalence of the GPF being positioned opposite to the third molar was 63.9% in a systematic review.³ In 73% of the South-Eastern European population the GPF was located internally from the third molar.¹⁰ Also, in 76.2%, the GPF were between proximal-distal surfaces of the third maxillary molar.²⁹ Furthermore, the GPF was opposite to the third molars in 73.75%,⁹ 74.6%,¹⁵ and 73.38% of cases in India.³⁰ On the other hand, in the South American (Brazil) population, the GPF was opposite to the third molars in 54.87% of the cases.¹¹ However, for more precise GPF positions, Ikuta et al.¹² used the CBCT technique and proposed a classification considering five tangents drawn parallel to the middle of and interproximal to the face of the upper molars adjacent to the third maxillary molars. This study found that 0% of the GPF was identified in position A and 3% of the GPF were identified from the centre of the second molar up to its distal face (position B), and 53% were identified from the medial surface of the third molar up to its centre (position C). As many as 39% were identified from the centre of the third molar up to its distal face (position D), and 5% were located from the distal to the third molar (position E). Therefore, 92% of the GPFs were located opposite to the third molar. Among Peruvian adults currently studied, the GPF was identified in positions B, C, D, and E at 19.42%, 68.94%, 7.76%, and 3.88%, respectively and none position A was found. Hence, 76.70% of the GPFs were located opposite to the third molar. These results accord with findings of other studies in the South American population. In 54.87% and 92% of Brazilians the GPFs were opposite to the third molars respectively.^{11, 12} In relation to these studies, two systematic reviews have confirmed the most frequent position of GPF was opposite to the third molars (63.9%)³ or in the midpalate area of the teeth (57.08%)³² of the global population.

On the other hand, the results of this present study did not show a significant difference in the GPF positions by gender as Ikuta et al.¹² and Aound et al.¹⁶ also found. Interestingly, there was no position A (from medial surface to the second molar) in the samples evaluated. These results are consistent with findings of studies conducted by Ikuta et al.¹²,

but Aound et al.¹⁶ have reported only 1.72% were identified using CBCT scans in Lebanese population. The GPF in the medial surface to the second molar was not found in Brazilian and Peruvian populations if scanned using CBCT. It is important to stress that this present study evaluated the Peruvian adult population aged 18-40, 41-60, and 61-77 years. Ikuta et al.¹² identified more precise GPF locations that position C was the most frequent in all age groups and had a significant association with age. Considering the findings, this study concludes position C from the medial surface of the third molar up to its centre (position C) is preferable to identify the positions of the GPF in this Peruvian adult population. Thus, these results are remarkable in performing surgical and anesthetic procedures.

Concerning the maxillary arch forms, this present study has discovered ovoid arches, followed by square and tapered shapes, were the most frequent form both in gender and age variables (50.49%). These findings are consistent with previous studies that have reported 41%, 42.4%, and 68% of ovoid arches were found in Saudi, Turkish, and Sudanese adult populations, respectively.³²⁻³⁴ In South American populations, Agurto et al.³⁵ evaluated the maxillary arches in Chilean children and reported ovoid arches mostly found in 50% of the samples. Additionally, Louly et al.³⁶ informed ellipse arches were discovered in 86.4% of Brazilian children. Although the arch forms were not associated with gender and age variables, the study has contributed to cover such topics that are still limited in the South American population. Besides, this study showed no significant association between the positions of the GPF and maxillary arch forms; thus, position C is not always frequent in ovoid arches. With that reason, clinicians should not consider arch forms when performing surgical procedures that depend on the positions of the GPF.

Despite the findings, this study only evaluated only one GPF location (right or left) because not all the samples had three molars in both locations. However, one study that used CBCT scans¹² and one study that used micro-CT⁷ for evaluating the positions of the GPF failed to find significant differences between right and left locations.

However, this study has brought CBCTs as an interesting tool for evaluating different

structures in the maxillomandibular regions. Therefore, it is recommended that future studies can investigate morphometric aspects of greater palatine canal, incisive foramen, lesser palatine canal, lesser palatine foramen, posterior nasal spine, pterygopalatine fossa, and midpalate fissure of South American populations to provide information for interventional procedures.

Conclusions

Based on the present investigation, maxillary arch forms had no association with the positions of the GPF. In a gingival graft surgery or anesthetic procedures, it should be noted the GPF is possibly located opposite to the third molar, specifically from the medial surface of the third molar up to its centre.

Future Scope / Clinical Significance

Clinician who performs gingival graft surgery or anesthesia procedures must know the anatomy of the palate such as the location of the greater palatine foramen (GPF) to avoid hemorrhagic risks and anesthesia failures. Although several information about the position of the GPF on dry skulls have been reported, the association of the GPF with other variables such as the maxillary arch shape is lacking.

Acknowledgements

The authors are grateful to the Ministry of Research, Technology and Higher Education, Indonesia and Faculty of Dental Medicine, Universitas Airlangga for the support this research could be conducted.

Declaration of Interest

The authors declare that there are no conflicts of interest.

Ethical policy and institutional review board statement: Ethical clearance of this retrospective study had been obtained from the Research Ethics Committee of the School of Dentistry of Universidad Científica del Sur, Lima-Perú with the approval number: 100002421.

References

1. Zucchelli G, Sharma P, Mounssif I. Esthetics in periodontics and implantology. *Periodontol* 2000. 2018;77(1):7-18.
2. Zucchelli G, Tavelli L, McGuire MK, et al. Autogenous soft tissue grafting for periodontal and peri-implant plastic surgical reconstruction. *J Periodontol* 2020;91(1):9-16.
3. Tomaszewska IM, Tomaszewski KA, Kmiołek EK, et al.

- Anatomical landmarks for the localization of the greater palatine foramen—a study of 1200 head CTs, 150 dry skulls, systematic review of literature and meta-analysis. *J Anat* 2014;225(4):419-435.
4. Norton NS. 2nd ed. Philadelphia: Elsevier Health Sciences; 2011. *Netter's Head and Neck Anatomy for Dentistry*: 553.
 5. Cagimni P, Govsa F, Ozer MA, Kazak Z. Computerized analysis of the greater palatine foramen to gain the palatine neurovascular bundle during palatal surgery. *Surg Radiol Anat* 2017;39(2):177-184.
 6. Gibelli D, Borlando A, Dolci C, Pucciarelli V, Cattaneo C, Sforza C. Anatomical characteristics of greater palatine foramen: a novel point of view. *Surg Radiol Anat* 2017;39(12):1359-1368.
 7. Beetge MM, Todorovic VS, Oettlé A, Hoffman J, van Zyl AW. A micro-CT study of the greater palatine foramen in human skulls. *J Oral Sci* 2018;60(1):51-56.
 8. Ajmani ML. Anatomical variation in position of the greater palatine foramen in the adult human skull. *J Anat* 1994;184(3):635-637.
 9. D'Souza AS, Mamatha H, Jyothi N. Morphometric analysis of hard palate in south Indian skulls. *Biomed Res* 2012;23(2):173-175.
 10. Nimigean V, Nimigean VR, Buşinciu L, Sălăvăstru DI, Podoleanu L. Anatomical and clinical considerations regarding the greater palatine foramen. *Rom J Morphol Embryol* 2013;54(Suppl 3):779-783.
 11. Chrcanovic BR, Custódio AL. Anatomical variation in the position of the greater palatine foramen. *J Oral Sci* 2010;52(1):109-113.
 12. Ikuta CR, Cardoso CL, Ferreira-Júnior O, Lauris JR, Souza PH, Rubira-Bullen IR. Position of the greater palatine foramen: an anatomical study through cone beam computed tomography images. *Surg Radiol Anat* 2013;35(9):837-842.
 13. Klosek SK, Rungruang T. Anatomical study of the greater palatine artery and related structures of the palatal vault: considerations for palate as the subepithelial connective tissue graft donor site. *Surg Radiol Anat* 2009;31(4):245-250.
 14. Wang TM, Kuo KJ, Shih C, Ho LL, Liu JC. Assessment of the relative locations of the greater palatine foramen in adult Chinese skulls. *Acta Anat (Basel)* 1988;132(3):182-186.
 15. Saralaya V, Nayak SR. The relative position of the greater palatine foramen in dry Indian skulls. *Singapore Med J* 2007;48(12):1143-1146.
 16. Aoun G, Nasseh I, Sokhn S, Saadeh M. Analysis of the greater palatine foramen in a Lebanese population using cone-beam computed tomography technology. *J Int Soc Prev Community Dent* 2015;5(Suppl 2):82-88.
 17. Noroozi H, Nik TH, Saeeda R. The dental arch form revisited. *Angle Orthod* 2001;71(5):386-389.
 18. Kook YA, Nojima K, Moon HB, McLaughlin RP, Sinclair PM. Comparison of arch forms between Korean and North American white populations. *Am J Orthod Dentofacial Orthop* 2004;126(6):680-686.
 19. Bae M, Park JW, Kim N. Semi-automatic and robust determination of dental arch form in dental cone-beam CT with B-spline approximation. *Comput Methods Programs Biomed* 2019;172(1):95-101.
 20. Diba SF, Azhari, Pramanik F, Tjahajawati S. Analysis of Beta-Crosslaps (B-Ctx) and Mandible Trabecular Parameters in Menopausal Women Using Cone Beam Computed Tomography (Cbct). *Journal of International Dental and Medical Research*. 2020;13(1): 189-93
 21. Azhari, Fahmi O, Fariska I. Normal Value of Cortical and Mandibular Trabecular Bone Density using Cone Beam Computed Tomography (CBCT). *Journal of International Dental and Medical Research*. 2019;12(1):160-4
 22. Pratiwi D, Soegiharto BM, Krisnawati, Kiswanjaya B. Orthodontists Reproducibility and Accuracy in Linear and Angular Measurement on 2d Digital and 3d Cbct Radiographic Examination. *Journal of International Dental and Medical Research*. 2017;10(3): 997-1004
 23. Chrystinasari NA, Narmada IB, Triwardhani A. Position of Unilateral / Bilateral Permanent Canine Impaction on the

- Prognosis of Treatment with KPG Index: 3D Cone Beam Computed Tomography Analysis. *Journal of International Dental and Medical Research*. 2021;14(4):1523-30
24. Das S, Kim D, Cannon TY, Ebert CS Jr, Senior BA. High-resolution computed tomography analysis of the greater palatine canal. *Am J Rhinol* 2006;20(6):603-608.
 25. Bahşi İ, Orhan M, Kervancıoğlu P, Yalçın ED. Morphometric evaluation and clinical implications of the greater palatine foramen, greater palatine canal and pterygopalatine fossa on CBCT images and review of literature. *Surg Radiol Anat* 2019;41(5):551-567.
 26. Fonseka MCN, Hettiarachchi PVKS, Jayasinghe RM, Jayasinghe RD, Nanayakkara CD. A cone beam computed tomographic analysis of the greater palatine foramen in a cohort of Sri Lankans. *J Oral Biol Craniofac Res* 2019;9(4):306-310.
 27. Hassanali J, Mwaniki D. Palatal analysis and osteology of the hard palate of the Kenyan African skulls. *Anat Rec* 1984;209(2):273-280.
 28. Langenegger JJ, Lownie JF, Cleaton-Jones PE. The relationship of the greater palatine foramen to the molar teeth and pterygoid hamulus in human skulls. *J Dent* 1983;11(3):249-256.
 29. Piagkou M, Xanthos T, Anagnostopoulou S, et al. Anatomical variation and morphology in the position of the palatine foramina in adult human skulls from Greece. *J Craniomaxillofac Surg* 2012;40(7):206-210.
 30. Sharma NA, Garud RS. Greater palatine foramen-key to successful hemimaxillary anaesthesia: a morphometric study and report of a rare aberration. *Singapore Med J* 2013;54(3):152-159.
 31. Tavelli L, Barootchi S, Ravidà A, Oh TJ, Wang HL. What is the safety zone for palatal soft tissue graft harvesting based on the locations of the greater palatine artery and foramen? A systematic review. *J Oral Maxillofac Surg* 2019;77(2):1-9.
 32. Mohammad A, Korlakunte PR. Gender identification and morphologic classification of tooth, arch and palatal forms in Saudi population. *J Pharm Bioallied Sci* 2015;7(Suppl 2):486-490.
 33. Celebi AA, Keklik H, Tan E, Ucar FI. Comparison of arch forms between Turkish and North American. *Dental Press J Orthod* 2016;21(2):51-58.
 34. Saeed HK, Mageet AO. Dental arch dimensions and form in a Sudanese sample. *J Contemp Dent Pract* 2018;19(10):1235-1241.
 35. Agurto P, Sandoval P. Morphology of the maxillary and mandibular arch in children of Mapuche and Non-Mapuche ancestry. *Int. J. Morphol* 2011;29(4):1104-1108.
 36. Louly F, Nouer PR, Janson G, Pinzan A. Dental arch dimensions in the mixed dentition: a study of Brazilian children from 9 to 12 years of age. *J Appl Oral Sci* 2011;19(2):169-174.